

УДК 532.528

DRAG DROP ON HIGH-SPEED SUPERCAVITATING VEHICLES AND SUPERSONIC SUBMARINES

I. NESTERUK

*[Institute of Hydromechanics, National Academy of Sciences of Ukraine, Kyiv
vul. Zheliabova, 8/4, 03680, Kyiv, Ukraine
E-mail: inesteruk@yahoo.com*

Отримано 10.11.2015

Supercavitation can significantly reduce the drag of high-speed underwater vehicles. To be located inside the cavity, the shape of the hull varies at different operating velocities and becomes very slender at high speeds. Simple estimations showed that at steady horizontal motion, the drag of a properly shaped supercavitating vehicle of a given volume decreases with increasing speed. This drag reduction opens up prospects for designing large high-speed underwater vehicles and even supersonic submarines.

KEY WORDS: *supercavitating vehicle, drag reduction, supersonic water flow*

Суперкавітація може суттєво знизити опір високошвидкісних підводних апаратів. Щоб корпус розташовувався всередині каверни, його форма має бути різною при різних швидкостях руху і стає дуже видовженою на великих швидкостях. Прості оцінки показали, що при усталеному горизонтальному русі опір відповідно сконструйованого суперкавітуючого апарата фіксованого об'єму зменшується зі зростанням швидкості. Це спадання опору відкриває перспективи створення великотоннажних високошвидкісних підводних апаратів і навіть надзвукових підводних човнів.

КЛЮЧОВІ СЛОВА: *суперкавітуючий апарат, зниження опору, надзвуковий потік води*

Суперкавітація может существенно снижать сопротивление высокоскоростных подводных аппаратов. Для размещения корпуса внутри каверны его форма должна изменяться при разных скоростях движения и становится очень удлиненной на больших скоростях. Простые оценки показали, что при установившемся горизонтальном движении сопротивление соответственно сконструированного суперкавитирующего аппарата уменьшается при возрастании скорости. Это падение сопротивления открывает перспективы создания крупнотоннажных высокоскоростных подводных аппаратов и даже сверхзвуковых подводных лодок.

КЛЮЧЕВЫЕ СЛОВА: *суперкавитирующий аппарат, снижение сопротивления, сверхзвуковое течение воды*

INTRODUCTION

The drag of underwater vehicles can be reduced by using the special shaped hulls without boundary layer separation (see Fig. 1a, [1, 2]) or by decreasing the area wetted by water, i.e., by the use of supercavitation (see Fig. 1b and 1c). In the case of supercavitation the main part of the hull is located inside the cavity, therefore the skin-friction drag can be significantly reduced, since the density of vapor or/and gas inside the cavity is approximately 800 time less than the water density ρ . This idea was developed in many theoretical, numerical and experimental investigations in many countries, [3-15]. In particular, the supersonic velocities (greater than the speed of sound $a \approx 1450$ m/s) were achieved for small supercavitating projectiles, launched by guns or special catapults [13-15].

Recently researchers in China are reporting that they have taken a big step towards creating a supersonic submarine. This technology could

theoretically get from Shanghai to San Francisco — about 6,000 miles — in just 100 minutes [16]. The supercavitating flow pattern shown in Figs. 1b, 1c yields a large pressure drag, because of the high pressure acting on the cavitator (a part of the hull, wetted by water). In this paper we will estimate this drag and discuss the possibility of constructing corresponding hulls and obtaining sufficient thrust to move a large vehicle at supersonic velocity.

1. PRESSURE DRAG ESTIMATIONS FOR DISC OR NON-SLENDER CONIC CAVITATORS

The pressure drag X for the steady horizontal supercavitating motion at velocity U can be expressed with the use of different drag coefficients, based on the vehicle volume V , the cavitator radius R_n and the depth of movement h (in meters):

$$X = 0.5C_V\rho U^2 V^{2/3} = C_{Vh}\rho g(h + 10)V^{2/3} =$$

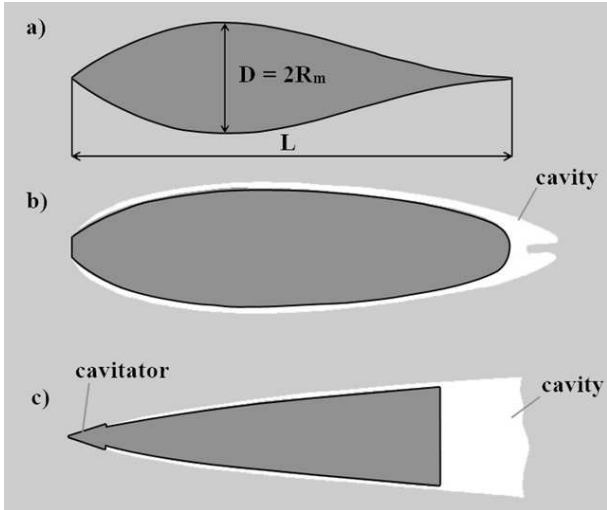


Fig. 1. Different axisymmetric underwater flow patterns:

- a) flow without boundary layer separation;
- b) supercavitating flow with a disc cavitator;
- c) supercavitating flow with a slender conical cavitator;

the hull is located in the nose part of the cavity only

$$= 0.5\pi C_x \rho U^2 R_n^2 \quad (1)$$

Here g is the acceleration of gravity.

For disc or non-slender conic cavitators (with the angle 2θ , $\theta > 25^\circ$) at subsonic velocities $U \ll a$, the semi-empiric Garabedian formulas, [17]:

$$R^2 = \frac{x(1-x)}{\lambda^2}, \quad \frac{R_n}{L} = \frac{\sigma}{2\sqrt{-C_x \ln \sigma}}, \quad (2)$$

$$\lambda = \frac{L}{D} = \sqrt{\frac{-\ln \sigma}{\sigma}}, \quad \frac{D}{R_n} = 2\sqrt{\frac{C_x}{\sigma}}$$

can be used to estimate the cavity shape at high Froude numbers. Here R is the cavity radius, based on the cavity length; λ is the cavity aspect ratio; D is the maximal cavity diameter; L is the cavity length; σ is the cavitation number; C_x is the pressure drag on the cavitator based on its area. The cavity volume can be obtained by integrating of the first eq. (2). Then for a vehicle which uses the cavity volume completely (as shown in Fig. 1b), the volumetric drag coefficient can be presented as follows, [18]:

$$C_V = \sqrt[3]{\frac{9\pi\sigma^4}{-16 \ln \sigma}}, \quad \sigma = \frac{2g(h+10)}{U^2}. \quad (3)$$

We consider only the case of vapor cavitation and neglect the pressure of vapor and gas inside the cavity in comparison with the ambient water pressure. For ventilated cavities (see, e.g., [9-11]) the gas pressure must be taken into account. For very high-speed vehicles moving at limited depth there is no need to use ventilation since the cavitation number is small and the cavity is large enough to locate the hull inside it. It must be noted that the value C_V does not depend on θ and tends to zero with diminishing of the cavitation number (or with increasing the velocity).

2. DRAG ESTIMATIONS ON SLENDER CAVITATORS IN COMPRESSIBLE FLUID

For the potential of the steady axisymmetric flow around a slender body, the Laplace equation can be represented as follows, [19]:

$$(1 - M^2) \frac{\partial^2 \Phi}{\partial x^2} + \frac{1}{r} \frac{\partial \Phi}{\partial r} + \frac{\partial^2 \Phi}{\partial r^2} = 0, \quad M = \frac{U}{a}$$

for both the subsonic $M < 0.9$, and the supersonic $M > 1.1$ cases (the transonic case needs a special treatment).

By means of the matched asymptotic expansion method identical to one presented in [20] or through the separation of the leading term of order $\varepsilon^2 \ln \varepsilon$ (ε is a small parameter, ratio of the maximum radius of the cavity or hull R_m to the length L , see Fig.1) in the corresponding expressions of the monograph [19], the following formulas for the flow potential can be obtained, [21, 22]:

$$\Phi(x, r, \varepsilon) = x + \varepsilon^2 \ln \varepsilon A(x) + \quad (4)$$

$$+ \varepsilon^2 \{A(x) \ln(\omega r_*) + B(x)\} + O(\varepsilon^4 \ln^2 \varepsilon)$$

$$r_* = \frac{r}{\varepsilon}; \quad A(x) = F \frac{dF}{dx}; \quad F(x) = \frac{R(x)}{\varepsilon}; \quad \varepsilon \ll \frac{1}{M}; \quad (5)$$

$$\omega = \sqrt{|M^2 - 1|}; \quad B(x) = -A(x) \ln 2 - I(x)$$

$$I(x) = \begin{cases} \frac{1}{2} \int_0^1 \frac{dA(\xi)}{d\xi} \operatorname{sgn}(x - \xi) \ln |x - \xi| d\xi, & M < 1, \\ \int_0^x \frac{dA(\xi)}{d\xi} \operatorname{sgn}(x - \xi) \ln |x - \xi| d\xi, & M > 1. \end{cases} \quad (6)$$

For the subsonic flows, eqs. (4) – (6) differ from Cole’s potential [20] only by the presence of the additional term $A(x) \ln \omega$. In the supersonic case there are some additional differences in the integral item (6). The substitution of eq. (4) into Bernoulli integral and neglecting the gravity forces yield

$$\begin{aligned} \varepsilon^2 \ln \varepsilon \frac{dA}{dx} + \varepsilon^2 \left[\frac{dA}{dx} \ln(\omega F) + \frac{dB}{dx} + \frac{A^2}{2F^2} \right] + \\ + O(\varepsilon^4 \ln^2 \varepsilon) = 0.5\sigma. \end{aligned} \tag{7}$$

Since eq. (7) is of the same structure as the corresponding equation in incompressible fluid, their solutions are identical in structure as well. With the use of asymptotical method, presented in [23], the first and second approximation equations can be written as follows:

$$\varepsilon^2 \frac{d^2 f_1}{dx^2} = \frac{d^2 R^2}{dx^2} = \frac{\sigma}{\ln \varepsilon}, \tag{8}$$

$$\begin{aligned} \frac{d^2 R^2}{dx^2} = \frac{\sigma}{\ln \varepsilon} - \frac{\varepsilon^2}{\ln \varepsilon} \left[\frac{dA_1}{dx} \ln(\omega^2 f_1) + \right. \\ \left. 2 \frac{dB_1}{dx} + \frac{A_1^2}{f_1} \right] + O\left(\frac{\varepsilon^2}{\ln^2 \varepsilon}\right). \end{aligned} \tag{9}$$

Here $A_1 = 0.5df_1/dx$ and the functions B_1, I_1 can be obtained from (5) and (6) through the substitution of A_1 for A .

The first approximation eq. (8) and its solution for the cavity radius (at $\varepsilon = \beta$)

$$\frac{R^2}{R_n^2} = \alpha \frac{x^2}{R_n^2} + 2\beta \frac{x}{R_n} + 1, \quad \alpha = \frac{\sigma}{2 \ln \beta}, \quad \beta = \text{tg}(\theta) \tag{10}$$

are valid for both sub- and supersonic velocities and coincide with the corresponding equation for the incompressible fluid, [24].

Equation (10) allows calculating the maximal cavity diameter D ; the cavity length L and the cavitator+cavity aspect ratio λ :

$$\bar{D} = \frac{D}{R_n} = 2\sqrt{1 - \frac{\beta^2}{\alpha}}, \tag{11}$$

$$\bar{L} = \frac{L}{R_n} = \frac{-\beta - \sqrt{\beta^2 - \alpha}}{\alpha}, \quad \lambda = \frac{\bar{L} + 1/\beta}{\bar{D}}.$$

The influence of the compressibility becomes perceptible only from the second approximation. The

analytical formulas for the second approximation are presented in [22, 25]. It was shown that for a subsonic flow of compressible imponderable fluid at $\sigma > 0$, the supercavity dimensions are greater than those in incompressible fluid ($M \rightarrow 0$). The most significant influence of the compressibility occurs as $U \rightarrow \alpha$. But the water compressibility extends the cavity sizes no more than by 10%.

In the supersonic case for positive values of the cavitation number in the Mach number range $1.1 \leq M \leq 1.3$, the dimensions of the cavity are greater than in incompressible fluid ($M \rightarrow 0$), whereas at $M \geq 1.5$ they become less. However, the deviations from the values describing the case of incompressible fluid do not exceed 10%.

In incompressible fluid the pressure drag of the conical cavitator is determined in [26] with the use of the first approximation for the cavity shape and is in a good agreement with the experimental data and numerical calculations. Since the first approximation of the cavity shape doesn’t depend on the Mach number (see (8), (10)), the method offered in [26] was simply generalized in [22, 25] for the case of compressible liquid and the following equation was obtained for the pressure drag coefficient of slender cones in the subsonic flows ($M < 0.9$):

$$C_x = C_{x0} + \sigma + \frac{\sigma(l^2 - l - 2l \ln l + l^2 \ln l - l_k^2 \ln l_k)}{2l_k^2 \ln \beta}, \tag{12}$$

$$l_k = \frac{1}{1 + \beta \bar{L}}, \quad l = 1 - l_k.$$

$$C_{x0} = -2\beta^2 \left(\ln \frac{\beta \omega}{2} + 1 \right). \tag{13}$$

In the supersonic case ($M > 1.1$), the drag on the cavitator doesn’t depend on the cavity shape and the following formulas can be obtained for the slender conical cavitators, [19, 22, 25]:

$$C_x = C_{x0} + \sigma, \quad C_{x0} = -2\beta^2 \left(\ln \frac{\beta \omega}{2} + \frac{1}{2} \right). \tag{14}$$

So, the compressibility of liquid influences only on the value C_{x0} which can be treated as a theoretical limit of the drag when $\sigma \rightarrow 0$. Specifically, for conic cavitator, this value C_{x0} is determined by eqs. (13) and (14) in the subsonic and supersonic cases, respectively. The numerical results based on formulae (13) and (14) are represented in Fig. 2 by lines for cones with different values of the angle 2θ . Some numerical results available in the literature are also

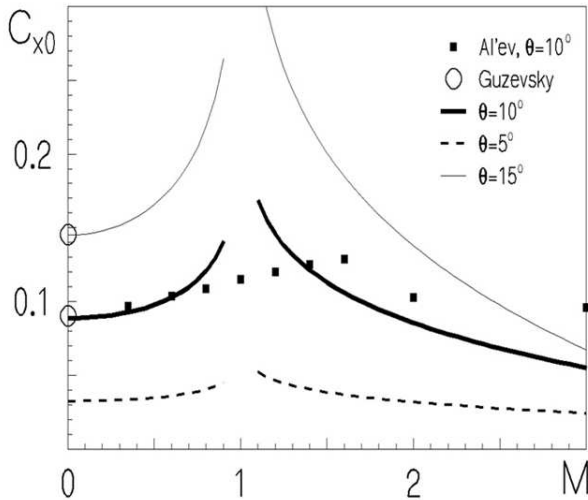


Fig 2. Calculations of the c_{x0} values for different conical cavitators. Slender body theory (eqs. (13) and (14), [22, 25]) are represented by lines, non-linear numerical methods [27, 28] – by markers

shown in Fig. 2 by markers. It can be seen that formulas (13) and (14), obtained with the use of the slender body theory, are in rather good agreement with the numerical non-linear calculations performed in [27, 28]. It should be noted that the drag increases as the Mach number is near 1.0. This tendency is significant for thicker cones. Thus, slender conical cavitators are preferable for supersonic vehicles (similar situation occurs in the case of supersonic airplanes, which have a sharp nose).

Knowing C_x , the drag coefficients C_V and C_{Vh} can be calculated with the use of eqs. (1), (10) and (12-14)

$$C_V = \pi C_x \left[\frac{R_n^3}{\gamma V_1} \right]^{2/3}, \quad C_{Vh} = \frac{0.5 C_V U^2}{g(h+10)}; \quad (15)$$

$$\frac{V_t}{R_n^3} = \pi \left(\frac{1}{3\beta} + \frac{\alpha}{3} \bar{L}^3 + \beta \bar{L}^2 + \bar{L} \right), \quad \gamma = \frac{V}{V_t} \leq 1,$$

where γ is the part of the cavitator+cavity volume V_t used to locate the hull. To estimate the additional laminar friction drag on the slender conical cavitator with the volume $V_b = \pi/(3\beta)$, the following formula was used, [29]:

$$\Delta C_V = \frac{4.708}{\sqrt{\text{Re}_V}} \sqrt{\frac{V_b}{V}}; \quad \text{Re}_V = \frac{UV^{1/3}}{\nu}. \quad (16)$$

3. RESULTS AND DISCUSSION

The results of calculations with the use of (11)-(16) are represented in Figs. 3 and 4. Fig. 3 shows that the volumetric drag coefficient slightly depends on the cavitator shape and increases with increasing the depth of horizontal movement. To compare with the laminar useparated flow pattern (as shown in Fig. 1a), formula (16) with $V_b = V$ and the water viscosity $\nu = 1.3 \cdot 10^{-6} \text{ m}^2/\text{s}$ was used for different values of the vehicle volume $V = 10^{-3}, 1, 10^3 \text{ m}^3$ (see dotted lines). It can be seen that supercavitation is preferable for small and very fast vehicles (the examples of the calculations of the critical hull volume are presented in [18]). Equation (16) yields estimation for the minimum possible drag of the attached flow pattern, since at large Reynolds numbers, the friction drag drastically increases due to the turbulence. The critical Reynolds number for the laminar-to-turbulent transition can be rather high for slender unseparated bodies, [30, 31], nevertheless at large subsonic and supersonic speeds the use of supercavitation is evidently preferable.

The C_{Vh} calculations (shown in Fig. 4) are very surprising, since drag of a supercavitating vehicle of a fixed volume (its hull shape is changeable to be located inside the cavity), moving at constant depth, decreases with the increasing the velocity (see dashed (disc or non-slender conical cavitator) and solid (slender conical cavitator, $\beta = 0.1$) lines). In particular, the drag of a proper shaped supersonic vehicle can be smaller than subsonic one. This feature is only inherent with supercavitation. In air (or in water without separation) the drag increases with speed.

At very high velocities the use of supercavitation is limited by the increase of the corresponding aspect ratio of the cavity (see dotted lines for the slender conical cavitator, $\beta = 0.1$). The aspect ratio of the vehicle λ_V - can be smaller than λ , but in this case only a part of the cavity volume is used to locate the hull (as shown in Fig. 1c), the value γ decreases and C_V and C_{Vh} increase (see eq. (15)). Thus, at very high speeds and small depths supercavitation requires very strong and slender hulls to withstand heavy longitudinal forces and to avoid buckling. To balance the weight of the supercavitating vehicle the corresponding lift force must be created with the use of planing or fins, piercing the cavity (see, e.g., [12]). Some estimations of the corresponding additional drag are presented in [18].

Let us estimate the thrust of a supersonic underwater submarine ($U = 1600 \text{ m/s}$; $V = 1000 \text{ m}^3$; $h = 10 \text{ m}$, $\beta = 0.1$; $\lambda_V = 80$, $\gamma = 0.5$)

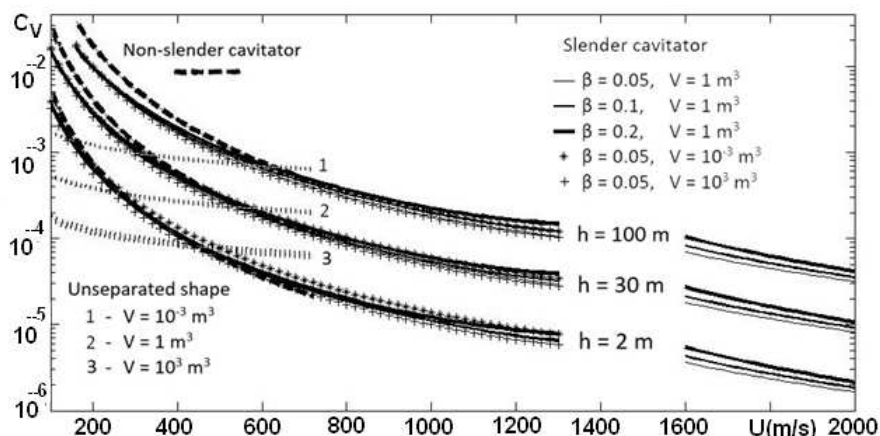


Fig 3. Volumetric drag coefficients for supercavitating (at different values of the depth h ; $\gamma = 1$) and attached flows. Disc and non-slender conical cavitators – eq. (3), dashed lines; slender conical cavitators, eqs. (11)-(16): solid lines $V = 1\text{ m}^3$; $\beta = 0.05; 0.1; 0.2$ (thickness decreases for slenderer ones); “stars” – $V = 10^{-3}\text{ m}^3; \beta = 0.05$; “crosses” – $V = 1000\text{ m}^3$; $\beta = 0.05$. Values of C_V for the laminar unseparated flow pattern (shown in Fig. 1a) are represented by dotted lines for $V = 10^{-3}, 1, 1000\text{ m}^3$ (the thickness is increasing with the vehicle volume; eq. (9), $V_b = V$)

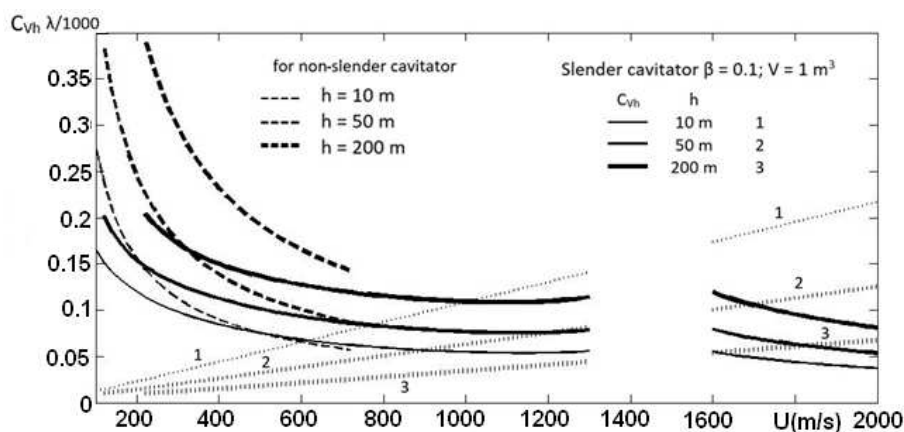


Fig 4. Drag coefficients C_{Vh} ($\gamma = 1$) and the cavator+cavity aspect ratio at different values of the depth $h = 10; 50; 200$ m (the thickness of the lines is increasing with the depth). C_{Vh} for disc and non-slender conical cavitators, eq. (3), (15) – dashed lines; for the slender conical cavitator, eqs. (11) – (15), $\beta = 0.1$; $V = 1\text{ m}^3$ - solid lines. Values $\lambda/1000$ for the slender conical cavitator, eq. (11), $\beta = 0.1$ -- dotted lines

which must be equal to the drag in the horizontal steady motion. We can expect a very small value of $C_V \approx 10^{-5}$, if its very slender hull is located inside the cavity (as shown in Fig. 1c). Then $X \approx 1280\text{ kN}$ and is comparable with the thrust of modern rocket engines. To estimate the range of such submarine let us use the relationship between the operation time T and the specific impulse I_{sp} and the mass m_f of the fuel: $T = I_{sp}m_f/X$. At $I_{sp} = 5000\text{ m/s}$ and $m_f = 10^6$ the operation time is approximately 3900 seconds and the range of the submarine is approximately 6250 km, i.e., comparable with the distance between Shanghai

and San-Francisco.

CONCLUSIONS

The drag of a supercavitating vehicle was estimated with the use of the slender body theory for sub- and supersonic velocities. The results are in rather good agreement with the known non-linear calculations. It was revealed that at steady horizontal motion, the drag of a properly shaped supercavitating vehicle of a given volume decreases with increasing

speed. This drag reduction opens up prospects for designing large high-speed underwater vehicles and even supersonic submarines, since the corresponding thrust values could be obtained with the use of modern rocket engines. To be located inside the cavity, the shape of the hull varies at different operating velocities and becomes very slender at high speeds. This fact creates challenges to strengthen the construction of the hulls in order to withstand heavy longitudinal forces and to avoid buckling.

1. *Nesteruk I.* Can Shapes with Negative Pressure Gradients Prevent Cavitation. FEDSM'034TH ASME - JSME Joint Fluids Engineering Conference Honolulu, Hawaii, USA, July 6–11, FEDSM2003 - 45323. – 2003.
2. *Nesteruk I.* Rigid Bodies without Boundary-Layer Separation// Int. J. of Fluid Mechanics Research. – 2014. –V. 41(3).– P. 260-281.
3. *Logvinovich G.V.* Hydrodynamics of Flows with Free Boundaries.–Halsted, 1973. – 208 p.
4. *Knapp R. T., Daily J. W. and Hammitt F. G.* Cavitation.– McGraw Hill, New York, 1970.– 688 p.
5. *Buyvol, V.N.* Oscillations and stability of deformed systems in fluid – Kiev: Naukova Dumka, 1975. – 192 p. (In Russian).
6. *Franc J.P. and Michel J.M.* Fundamentals of Cavitation, Kluwer, Dordrecht. – 2004.
7. *Nesteruk, I. ed.* Supercavitation. Advances and Perspectives. – Springer. – 2012. – 230p.
8. *Cameron P. J. K., Rogers P. H., Doane J. W. and Gifford D. H.* An Experiment for the Study of Free-Flying Supercavitating Projectiles// J. Fluids Eng., doi:10.1115/1.4003560. – V. 133(2).– 2011.
9. *Wosnik M. and Arndt R. E. A.* Measurements in High Void-Fraction Bubbly Wakes Created by Ventilated Supercavitation//J. Fluids Eng. Paper No: FE-12-1230; doi: 10.1115/1.4023193.– V. 135(1). – 2013.
10. *Huang Yu. X., Ch., Du, T., Liao, L., Wu, X., Zheng Zh. and Wang Y.* Study of Characteristics of Cloud Cavity Around Axisymmetric Projectile by Large Eddy Simulation//J. Fluids Eng. Paper No: FE-13-1216; doi: 10.1115/1.4026583. – 2014.– V. 136(5).
11. *Rashidi I., Passandideh-Fard Mo., Pasandideh-Fard Ma. and Nouri N. M.* Numerical and Experimental Study of a Ventilated Supercavitating Vehicle// J.Fluids Eng. Paper No: FE-13-1289; doi: 10.1115/1.4027383. – 2014.– V. 136(10).
12. *Zou W. and Liu H.* Modeling and Simulations of the Supercavitating Vehicle With Its Tail-Slaps//J. Fluids Eng. Paper No: FE-14-1007; doi: 10.1115/1.4029330. – 2015.– V. 137(4).
13. *Kirschner I. N.* Results of Selected Experiments Involving Supercavitating Flows// VKI/RTO Special Course on Supercavitation. Brussels: Von Karman Institute for Fluid Dynamics. – 2001.
14. *Savchenko Yu. N.* Perspectives of the Supercavitation Flow Applications// Int. Conf. on Superfast Marine Vehicles Moving Above, Under and in Water Surface (SuperFAST'2008), 2–4 July 2008. St. Petersburg, Russia.– 2008.
15. *Savchenko, Yu.N., Zverkhovskiy, A.N.* Procedure of experimental study of the high-speed motion of supercavitating inertial models in water // Applied Hydromechanics – 2009.– V. 11(4), – P. 69–75. (In Russian).
16. <http://www.extremetech.com/extreme/188752-chinas-supersonic-submarine-which-could-gofrom-shanghai-to-san-francisco-in-100-minutes-creeps-ever-closer-to-reality>
17. *Garabedian P.R.* Calculation of Axially Symmetric Cavities and Jets// Pac. J. Math.– 1956.– V. 6(4). – P. 611 - 684.
18. *Nesteruk I.* Drag Effectiveness of Supercavitating Underwater Hulls// in: Supercavitation, I. Nesteruk, Ed. Springer, – 2012. – P. 79 – 106.
19. *Frankl F. I. and Karpovich E. A.* Gas Dynamics of Thin Bodies, Interscience Pub., New York. – 1953.– 175p.
20. *Cole J. D.* Perturbation Methods in Applied Mathematics, Blaisdell Pub. Co.: Waltham, London. – 1968.– 274p.
21. *Nesteruk, I.* Body forms of minimal drag// Dopovidi AN Ukr.SSR, ser. A – 1989. – N 4 – P. 57-60. (In Ukrainian).
22. *Nesteruk I.* Influence of the Flow Unsteadiness, Compressibility and Capillarity on Long Axisymmetric Cavities// Fifth Int. Symposium on Cavitation (Cav2003), Osaka, Japan.– 2003.
23. *Nesteruk I.* Determination of the Form of a Thin Axisymmetric Cavity on the Basis of an integrodifferential equation// Fluid Dynamics, DOI: 10.1007/BF01050087 – 1985.– V. 20(5).– P. 735-741.
24. *Nesteruk I.* On the Shape of a Slender Axisymmetric Cavity in a Ponderable Liquid// Fluid Dynamics. DOI: 10.1007/BF01052000. –1979.– V.14(6). – P. 923 - 927.
25. *Nesteruk I.* Calculation of steady axisymmetric supercavity flows of compressible fluid// Bulletin of Univ. of Kiev, Ser.: Phys. and Math. – 2003. – N 4, P. 109 - 118.(In Ukrainian).
26. *Nesteruk I.* Some Problems of Axisymmetric Cavitation Flows// Fluid Dynamics. DOI: 10.1007/BF01090694. –1982. – V.17(1). – P. 21 - 27.
27. *Guzevsky L. G.* Numerical Analysis of Cavitation Flows. Preprint N 40-79 of SB AS USSR. Novosibirsk: Heat-Physics Institute (In Russian). – 1979.
28. *Al'ev G. A.* Transonic separation flow of water past a circular cone// Fluid Dynamics. – 1983. – V. 18(2). – P. 296 - 299.
29. *Buraga O.A., Nesteruk I.G. and Savchenko Yu. N.* Comparison of Slender Axisymmetric Body Drag Under Unseparated and Supercavitational Flow Regimes// Int. J. Fluid Mechanics Research. – 2006. – V. 33(3). – P. 255 - 264.
30. *Nesteruk I.* Peculiarities of Turbulization and Separation of Boundary-Layer on Slender Axisymmetric Subsonic Bodies// Naukovi visti, NTUU "Kyiv Polytechnic Institute" – 2002. – N3, –P. 70-76. (In Ukrainian).
31. *Nesteruk, I., Passoni G. and Redaelli A.* Shape of Aquatic Animals and Their Swimming Efficiency//J. Marine Biology, Article ID 470715, doi:10.1155/2014/470715. – 2014.